P H Y S I C A L R E V I E W L E T T E R S

Electronic Origins of Structural Distortions in Post-Transition Metal Oxides: Experimental and Theoretical Evidence for a Revision of the Lone Pair Model

D. J. Payne,[1] R. G. Egdell,[1,*] A. Walsh,[2] G. W. Watson,[2] J. Guo,[3] P.-A. Glans,[4] T. Learmonth,[4] and K. E. Smith[4]

[1]*Department of Chemistry, Inorganic Chemistry Laboratory, South Parks Road, Oxford OX1 3QR, United Kingdom*
[2]*Department of Chemistry, Trinity College, Dublin 2, Ireland*
[3]*Advanced Light Source, Lawrence Berkeley National Laboratory, Berkeley, California 94720, USA*
[4]*Department of Physics, Boston University, 590 Commonwealth Avenue, Boston, Massachusetts 02215, USA*
(Received 15 September 2005; published 19 April 2006)

Structural distortions in post-transition metal oxides are often explained in terms of the influence of sp hybrid "lone pairs." Evidence is presented here showing that this model must be revised. The electronic structures of prototypically distorted α-PbO and α-Bi$_2$O$_3$ have been measured by high-resolution x-ray photoemission and soft x-ray emission spectroscopies. In contrast with the expectations of the lone pair model, a high density of metal 6s states is observed at the bottom of the valence band. The measurements are consistent with the results of density functional theory calculations.

PACS numbers: 78.70.En, 79.60.−i

The heavier post-transition elements such as Tl, Pb, and Bi have two important oxidation states: the group state N and the N-2 state. The crystal structures of N-2 compounds frequently (but not always) involve irregular and noncentrosymmetric coordination environments for the metal cations: the oxides α-PbO and α-Bi$_2$O$_3$ are typical in this respect [1]. Thus tetragonal α-PbO (litharge) adopts a structure where four nearest neighbor oxygen atoms form a square on one side of the Pb atoms with four more distant oxygen atoms also in a square arrangement. The local coordination environment for Pb is of C_{4v} symmetry. In monoclinic α-Bi$_2$O$_3$ the two distinct Bi ions both have five oxygen near neighbors. This gives a distorted square pyramidal coordination geometry, again approximating to local C_{4v} symmetry, with a sixth more distant oxygen ion [1]. Gas-phase N-2 cations have a formal $6s^2$ electron configuration and because it is possible to achieve an N valence state, it is often assumed that the 6s electrons must lie close to the Fermi energy (E_F) in the solid state [2]. Distorted structures are then rationalized in terms of a metal 6s-6p hybrid "lone pair" orbital which is projected out into the void space within the distorted crystal structure [3–6]. Of course an isolated $6s^2$ cation is spherical. However, the lack of inversion symmetry at the metal sites within a typical N-2 structure allows mixing between occupied metal 6s states close to E_F and nominally unoccupied metal 6p states at higher energy, thus lowering the internal electronic energy of the metal cation through a second order Jahn-Teller mechanism and giving a directional s-p hybrid orbital. Such mixing is not possible at sites that possess inversion symmetry because s and p orbitals have different parity. There is, therefore, a driving force for structural distortion. This model has formed the basis for much recent discussion of the structural distortions found in ferroelectric oxides containing Pb(II) or Bi(III) [6].

The conventional lone pair model has, however, recently been called into question on the basis of density functional calculations which suggest that the majority of the 6s population in α-PbO is, in fact, found at the *bottom* of the main valence band, about 10 eV below E_F [7–9]. Significant mixing between Pb 6s and O 2p states exists, giving rise to a filled antibonding state with *some* 6s character at the top of the valence band, but it is not the energy where the majority of the 6s population is found. Further mixing between the antibonding state and nominally empty Pb 6p states is responsible for the distortion of PbO away from the closely related but higher symmetry CsCl structure. The asymmetric electron density therefore arises predominantly from a mix of O 2p and Pb 6p orbitals at the top of the valence band, in contrast to the conventional model of a purely metal-based 6s-6p lone pair. However, definitive experimental evidence to support these ideas has been lacking to date.

In the present communication we show that consideration of the relative intensities of valence band components in O K shell x-ray emission spectra provides a simple but incisive experimental approach to investigate the nature of lone pair states in metal oxides, especially when comparison is made with the intensities of spectral features in Al $K\alpha$ x-ray photoemission spectra. We report results first for α-PbO, where our data clearly show that states at the bottom of the valence band have a minority O 2p contribution and are therefore of predominant Pb 6s character. The validity of our ideas is confirmed by studying α-Bi$_2$O$_3$, where the lowest valence band state is found to be even more purely 6s-like. The experimental data are then compared to the results of calculations of the electronic structure of these materials performed using density functional theory.

Phase pure α-PbO was prepared by decomposition of β-PbO$_2$ at 572 °C [5]. The α-PbO was pelletized between tungsten carbide dies at 2 MT and sintered at 350 °C. α-Bi$_2$O$_3$ was obtained commercially (Aldrich 99.99%), pressed into pellets at 5 MT and sintered at 700 °C. In both cases the phase integrity of the resulting ceramic pellets was confirmed by x-ray diffraction.

High-resolution x-ray photoemission spectroscopy (XPS) measurements were performed using a Scienta ESCA 300 spectrometer at the National Centre for Electron Spectroscopy and Surface Analysis (NCESS) at Daresbury Laboratory (UK). The effective instrument energy resolution was 0.35 eV. Samples were cleaned *in situ* by rear face electron beam heating at 400 °C for PbO and 600 °C for α-Bi$_2$O$_3$. The C 1s to O 1s XPS core level intensity ratio was reduced to below 0.01 by this procedure. Sample charging was problematic and it was necessary to stabilize the surface charge with an electron flood gun. Binding energies were referenced to the residual C 1s peak, which was assigned to a binding energy of 285.0 eV.

X-ray absorption spectroscopy and x-ray emission spectroscopy (XES) experiments were performed on beam line 7.0.1 at the Advanced Light Source (ALS), Lawrence Berkeley National Laboratory, USA. This beam line is equipped with a spherical grating monochromator [10]. Emission spectra were recorded using a Nordgren-type grazing-incidence spherical grating spectrometer [11]. For the emission experiments, the beam line and the spectrometer were both set to have an energy resolution of 0.5 eV at the O K edge.

For comparison with the experimental data, density functional theory (DFT) as embodied in the Vienna *ab initio* Simulation Package (VASP) [12,13] was used to calculate the electronic structure of α-PbO and α-Bi$_2$O$_3$. The crystal wave functions were expanded in terms of a plane wave basis set using periodic boundary conditions with a plane wave cutoff of 500 eV and a k-point grid density of $6 \times 6 \times 6$ for α-PbO and $4 \times 4 \times 4$ for α-Bi$_2$O$_3$. The generalized gradient approximation parameterization of Perdew, Burke, and Ernzerhof [14] was used

with the projector augmented wave method employed to represent the valence-core interactions [15] (Pb, Bi: [Xe]; O: [He]). These fixed core states were generated from all-electron scalar relativistic calculations. The metal 5d states were included explicitly in the calculations, but the extent of hybridization of these states with O 2p states was negligible. In contrast to previous *ab initio* studies [16,17], optimization of atomic positions, lattice vectors, and bond angles was performed. The optimized Pb-O bondlength in α-PbO was within 1.3% of the experimental value, while for α-Bi$_2$O$_3$ (where there are ten distinct Bi-O bondlengths) the agreement was better than 3.0%. Both materials were found to be highly covalent with charges derived from Bader population [18] analyses of the electron densities of only $+1.15e$ and $+1.78e$ on the Pb(II) and Bi(III) cations, respectively.

Valence band XPS spectra of α-PbO and α-Bi$_2$O$_3$ are shown in the top left panel of Figs. 1 and 2, respectively, alongside calculated total densities of states derived from the DFT calculations. The XPS data for both α-PbO and α-Bi$_2$O$_3$ are in agreement with previously published data [16,19] but show better signal to noise and much better definition of the spectral features. For each oxide it is convenient to discuss the structure of the valence band in terms of three features, labeled I, II, and III. For α-PbO the low binding energy peak I apparently consists of two overlapping components with indication of a high binding energy shoulder. Peak II appears as a well-defined high binding energy shoulder to I, while peak III, which appears at the highest binding energy of 8.4 eV, is well-resolved from the rest of the valence band and shows signs of a low binding energy shoulder. The same basic spectral features are found for α-Bi$_2$O$_3$, although peak I is now split into
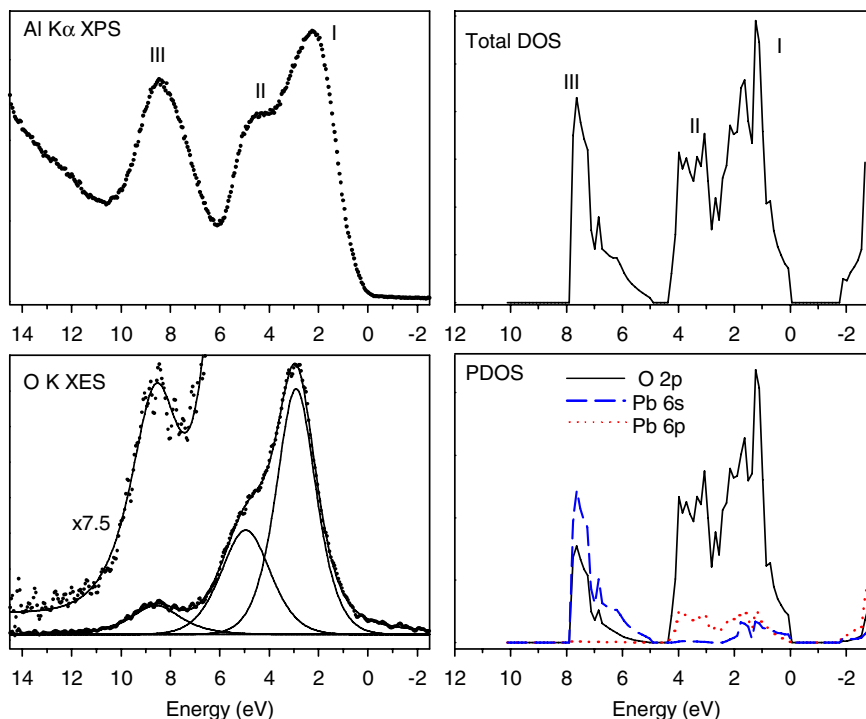

FIG. 1 (color online).   Valence band Al $K\alpha$ XPS and O K shell XES spectra from α-PbO compared with the total DOS and the PDOSs derived from DFT bandstructure calculations. The spectra are all presented on a binding energy scale referenced to the top of the valence band. XPS and XES spectra are aligned relative to each other using peak III. The overall spread of energies is 17 eV in the experimental spectra but only 15 eV in the calculated DOS.
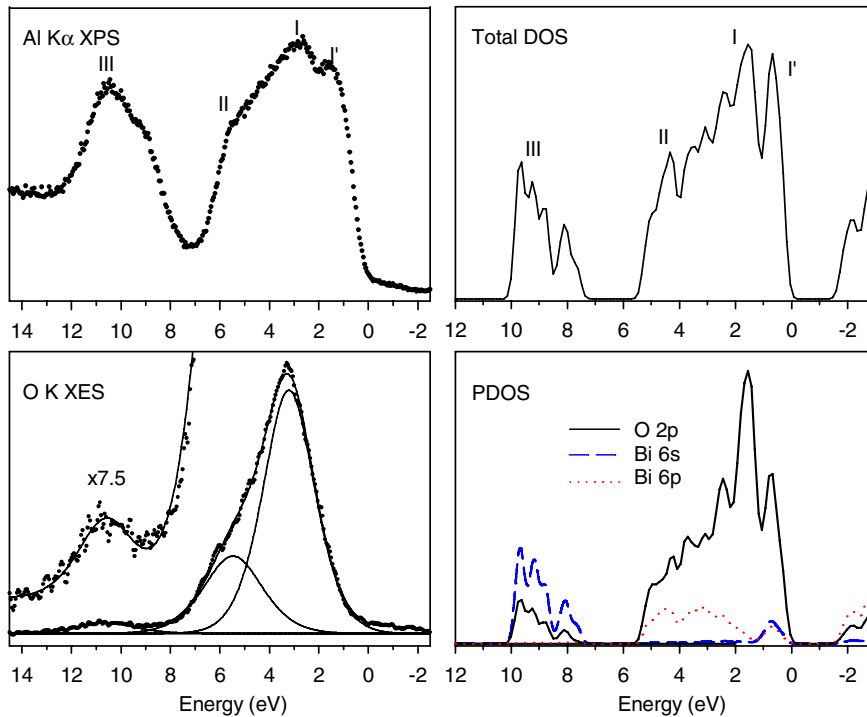
FIG. 2 (color online).   Valence band Al $K\alpha$ XPS and O K shell XES spectra from α-Bi_2O_3 compared with the total DOS and the PDOS derived from DFT bandstructure calculations. Alignments and energy scales as in Fig. 1.

two well-defined components. Moreover the band III shows a pronounced shift to the higher binding energy of 10.5 eV and the incipient splitting to reveal a low binding energy shoulder is better defined than in α-PbO. All of these features are reproduced in the band structure calculations shown in Figs. 1 and 2, including the splitting of peaks I and III for α-Bi_2O_3. The only discrepancy is that the overall energy spread of valence band states is less in the calculations than is found experimentally. This is a general problem when comparing densities of states (DOS) derived from DFT calculations with those from experimental photoemission spectra [20]. For these oxides XPS appears to measure the total DOS, suggesting that cross sections for ionization of O $2p$, Pb (Bi) $6s$, and Pb (Bi) $6p$ states are all very similar. This conclusion is in not in accord with the widely used ionization cross sections of Yeh and Lindau, where the Pb (Bi) $6p$ and $6s$ one electron ionization cross sections are calculated to be much larger than the O $2p$ cross section [21]. This highlights a difficulty in using XPS data alone to try to derive information about partial densities of states (PDOS).

O K shell emission spectra of the two oxides are shown in the lower left hand panels of Figs. 1 and 2. Again it is possible to identify three bands. There are, however, very pronounced changes in relative intensities as compared with the XPS data. Most strikingly the high binding energy band III is very much weaker relative to I and II in XES as compared with XPS. Because of the localized nature of the O $1s$ core hole and the dipole selection rule operative in x-ray emission, the O K shell emission spectra involve decay from occupied states of O $2p$ character into an O $1s$ core hole. O K emission therefore directly measures the O $2p$ PDOS. Thus the diminution of intensity of band III is a

clear signature of the fact that the corresponding electronic states at the bottom of the valence band have less O $2p$ character than the states closer to E_F.

To quantify this idea, it is possible to make an estimate of the O $2p$ contribution f_{O2p} to the lowest valence band state from the XES data as follows. Integration of the calculated density of states across band III reveals that it corresponds to two electron states per metal atom for both PbO and Bi_2O_3. If *all* the states in the valence band were of pure O $2p$ character it follows that the intensity of band III I_{III} relative to that of the total valence band I_{total} would simply be n/p where n is the number of metal atoms per formula unit and p is the total number of valence electron pairs per formula unit ($n = 1$, $p = 4$ for PbO; $n = 2$, $p = 11$ for Bi_2O_3) It follows that the fractional contribution of O $2p$ states to the lowest valence band f_{O2p} may be estimated from the ratio between the intensity I_{III} of the lowest valence band peak measured in XES and the total experimental valence band intensity I_{total}:

$$f_{O2p} = \frac{(I_{III}/I_{total})}{(n/p)}.$$

The results of this analysis for PbO and Bi_2O_3 are shown in Fig. 3, along with data for HgO, Tl_2O_3, and PbO_2 [22,23]. Corresponding values obtained by integrating the partial density of states from the DFT calculations are also shown. Both the experimental and calculated data clearly show that there is a progressive decrease in the amount of O $2p$ character in the valence band state at highest binding energy in moving across the periodic table. For both the lead oxides (PbO and PbO_2) and for Bi_2O_3 there is in fact less than 50% O $2p$ character present. Empirically we can
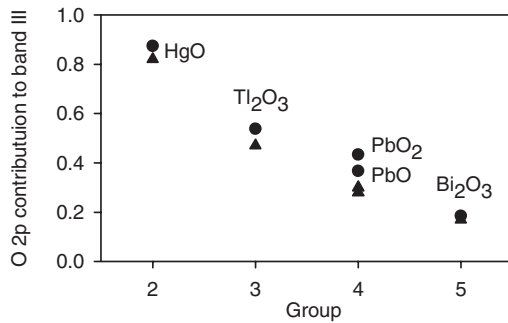
FIG. 3.   Closed circles: estimated O $2p$ contribution to the lowest valence band state derived from intensities in O K shell XES spectra of the post-transition metal oxides HgO, Tl_2O_3, PbO_2, PbO, and Bi_2O_3 as a function of group number. Triangles: the ratio $I(O2p)/\{I(O2p) + I(M6s)\}$ derived by integrating partial densities from DFT calculations across the lowest valence band state.

therefore deduce that the state at the bottom of the valence band must have dominant metal $6s$ atomic character. The empirical values depicted in Fig. 3 assume that the states in bands I and II are of pure O $2p$ atomic character. There is, in fact, some mixing of $6s$ and $6p$ character into these states, although Figs. 1 and 2 show that the extent of the mixing is quite small. Nonetheless due to this mixing the experimental values displayed in Fig. 3 must overestimate the true amount of O $2p$ character in the lowest valence band state. This accounts for the small systematic discrepancy between experimental and theoretical values.

In summary, our results indicate that the structural distortions found for α-PbO and α-Bi_2O_3 should not be attributed to direct mixing between cation levels close to the Fermi energy to give purely metal-based $6s$-$6p$ lone pairs. The dominant contribution to the metal $6s$ PDOS is found at the *bottom* rather than the *top* of the valence band and *indirect* mixing between $6s$ and $6p$ states is mediated by hybridization with O $2p$ states at the top of the valence band. It follows that qualitative textbook explanations of structural distortions in Pb(II) and Bi(III) compounds should be revised, with important implications in understanding the structural physics of, for example, magnetic ferroelectric materials such as $BiMnO_3$ [24] and $BiFeO_3$ [25]. Our results are also of general significance in relation to the electronic structures of ternary Pb(II) and Bi(III) oxides, including the many high temperature superconducting phases that contain these heavy cations. It has in the past been assumed that the $6s$ states lie close to E_F and therefore contribute significantly to the states responsible for conduction in metallic phases [2,26]. The present findings demonstrate that this viewpoint is not correct. Again this will impact understanding and tuning of the physical properties of these and related materials.

*Corresponding author.
Email address: russell.egdell@chem.ox.ac.uk
[1] A. F. Wells, *Structural Inorganic Chemistry* (Clarendon Press, Oxford, 1984).
[2] H. Namatame, A. Fujimori, H. Takagi, F. F. M. deGroot, and J. C. Fuggle, Phys. Rev. B **48**, 16 917 (1993).
[3] J. D. Dunitz and L. E. Orgel, Adv. Inorg. Chem. Radiochem. **2**, 1 (1960).
[4] D. M. Adams, *Inorganic Solids* (John Wiley, London, 1974).
[5] D. Le Bellac, J. M. Kiat, P. Garnier, H. Moudden, Ph. Sciau, P. A. Buffat, and G. André, Phys. Rev. B **52**, 13 184 (1995).
[6] B. B. Van Aken, T. T. M. Palstra, A. Filippetti, and N. A. Spalding, Nat. Mater. **3**, 164 (2004).
[7] G. W. Watson, S. C. Parker, and G. Kresse, Phys. Rev. B **59**, 8481 (1999).
[8] G. W. Watson and S. C. Parker, J. Phys. Chem. B **103**, 1258 (1999).
[9] A. Walsh and G. W. Watson, J. Solid State Chem. **178**, 1422 (2005).
[10] J. Nordgren and R. Nyholm, Nucl. Instrum. Methods Phys. Res., Sect. A **246**, 242 (1986).
[11] J. Nordgren, G. Bray, S. Cramm, R. Nyholm, J. E. Rubensson, and N. Wassdahl, Rev. Sci. Instrum. **60**, 1690 (1989).
[12] G. Kresse and J. Hafner, Phys. Rev. B **49**, 14 251 (1994).
[13] G. Kresse and J. Furthmuller, Comput. Mater. Sci. **6**, 15 (1996).
[14] J. P. Perdew, K. Burke, and M. Ernzerhof, Phys. Rev. Lett. **77**, 3865 (1996).
[15] P. E. Blöchl, Phys. Rev. B **50**, 17 953 (1994).
[16] H. J. Terpstra, R. A. de Groot, and C. Haas, Phys. Rev. B **52**, 11 690 (1995).
[17] J. M. Carlson, B. Hellsing, H. S. Domingos, and P. D. Bristow, Phys. Rev. B **65**, 205122 (2002).
[18] R. Bader, *Atoms in Molecules: A Quantum Theory* (Oxford University Press, New York, 1990).
[19] T. P. Debies and J. W. Rabalais, Chem. Phys. **20**, 277 (1977).
[20] Y. Dou, R. G. Egdell, D. S. L. Law, N. M. Harrison, and B. G. Searle, J. Phys. Condens. Matter **10**, 8447 (1998).
[21] J. J. Yeh and I. Lindau, At. Data Nucl. Data Tables **32**, 1 (1985).
[22] P. A. Glans, T. Learmonth, C. McGuinness, K. E. Smith, J. Guo, A. Walsh, G. W. Watson, and R. G. Egdell, Chem. Phys. Lett. **399**, 98 (2004).
[23] P. A. Glans, T. Learmonth, K. E. Smith, J. Guo, A. Walsh, G. W. Watson, F. Terzi, and R. G. Egdell, Phys. Rev. B **71**, 235109 (2005).
[24] R. Seshadri and N. A. Hill, Chem. Mater. **13**, 2892 (2001).
[25] J. Wang *et al.*, Science **299**, 1719 (2003).
[26] J. B. Goodenough, J. Gopalakrishnan, and K. Ramesha, J. Solid State Chem. **138**, 369 (1998).